Journal of Adhesion Science and Technology

ISSN: (Print) (Online) Journal homepage: https://www.tandfonline.com/loi/tast20

Effect of graphene on the mechanical and electrochemical properties of GLARE

Shuo Wang, Fanglin Cong, Sherif Araby, Saleh Kaytbay, Rui Cai, Xu Cui & Qingshi Meng

To cite this article: Shuo Wang, Fanglin Cong, Sherif Araby, Saleh Kaytbay, Rui Cai, Xu Cui & Qingshi Meng (2022) Effect of graphene on the mechanical and electrochemical properties of GLARE, Journal of Adhesion Science and Technology, 36:20, 2159-2175, DOI: 10.1080/01694243.2021.2003159

To link to this article: https://doi.org/10.1080/01694243.2021.2003159

Published online: 15 Nov 2021.

JOURNAL OF ADHESION SCIENCE AND TECHNOLOGY
2022, VOL. 36, NO. 20, 2159–2175
https://doi.org/10.1080/01694243.2021.2003159

Effect of graphene on the mechanical and electrochemical properties of GLARE

Shuo Wang[a,b], Fanglin Cong[c], Sherif Araby[d], Saleh Kaytbay[e], Rui Cai[f], Xu Cui[c] and Qingshi Meng[a]

[a]College of Aerospace Engineering, Shenyang Aerospace University, Shenyang, China; [b]School of Mechatronics, Northwestern Polytechnical University, Xian, China; [c]College of Civil Aviation, Shenyang Aerospace University, Shenyang, China; [d]School of Engineering and Digital Sciences, Nazarbayev University, Nur-Sultan, Kazakhstan; [e]Department of Mechanical Engineering, Benha Faculty of Engineering, Benha University, Benha, Egypt; [f]School of Mechanical, Aerospace and Automotive Engineering, Coventry University, Coventry, United Kingdom

ABSTRACT

This study explores the effect of different graphene contents on the mechanical behaviour, tensile and flexural properties, and the electrochemical performance of cross-layered glass-reinforced aluminium (GLARE) laminates. Results show that the mechanical properties of GLARE with different graphene contents are similar but not identical. The mass fraction of graphene (0 wt.%–1.0 wt.%) is calculated from the total mass of adhesive. As the graphene content increases (0 wt.%–1.0 wt.%), flexural strength peaks in the presence of 0.5 wt.% graphene, but tensile strength continues to increase. When the graphene mass ratio is 1.0 wt.%, the maximum tensile strength is 245.45 MPa. When the graphene mass ratio is 0.5 wt.%, interlaminar shear strength and flexural strength are 19.06 and 260.22 MPa, respectively, which correspond to different span–thickness ratios of 8/1 and 32/1. This graphene mass ratio indicates the best three-point flexural performance of graphene-reinforced GLARE. This study further explains the enhancement mechanism through fracture surface observation. Graphene with a mass ratio of 0.5 wt.% maximises the flexural strength whilst maintaining a strong GLARE electrochemical performance. At scanning speeds of 40, 80, and 100 mV/s, the specific capacitance values are 1.76, 2.47, and 2.88 F/g, respectively. According to quantum tunnelling theory, graphene can form a conductive network when it is dispersed in a resin matrix. This theory reveals the reason why 0.5 wt.% graphene platelet-modified GLARE has good electrochemical properties.

ARTICLE HISTORY
Received 9 August 2021
Revised 30 October 2021
Accepted 2 November 2021

KEYWORDS
GLARE; mechanical properties; electrochemical performance; graphene

1. Introduction

With the emergence and application of fibre metal laminates (FMLs), which is composed of alternating metal layers and fibre-reinforced composite layers, lightweight and high-performance materials have been developed [1,2]. One of the well-known FMLs is

CONTACT Xu Cui 19941821@sau.edu.cn; Qingshi Meng mengqingshi@hotmail.com

glass-reinforced aluminium (GLARE) [3]. GLARE laminates have a combination of the advantages of aluminium alloy and glass fibre-reinforced composite; some of these advantages are fatigue resistance [4], impact resistance [5], thermal ageing resistance [6]. As such, the performance of FMLs is further enhanced by exploring new methods. Nevertheless, the most common and effective method is the addition of nanofillers to a resin matrix [6–8].

Nanofiller incorporation can significantly influence the physical, chemical and mechanical properties of GLARE. Various nanofillers have different effects on materials [6,7,9–11]. In a previous study, inorganic nanofillers are added to the treatment of a metal surface, and its result shows that nano metal powders can significantly enhance the mechanical properties of GLARE; conversely, the enhancement effect of nano-level metal oxides is poor. The addition of nanoclay has a negative effect [9,12]. Multiwalled carbon nanotubes improve the shear strength of titanium-based FMLs by 87.5% [7,13]. Si-type nanofillers can enhance the thermal ageing resistance whilst improving the mechanical properties of GLARE. Silicon carbide addition can produce multifunctional GLARE with improved thermal resistance and performance [6]. Graphene oxide (GO) has a remarkable reinforcing effect on the tensile, bending properties and interlayer toughness of FMLs [10,11]. Specifically, GO (1.5 wt.%) improves tensile strength and flexural strength by 11.7% and 134.0%, respectively [10]. The synergistic effect of 0.5 wt.% GO and metal surface treatment methods enhance the interlaminar fracture toughness of modes I and II by 510% and 381%, respectively [11]. As a graphene derivative, GO is similar but not identical to graphene mainly because the functional group slightly damages the graphene lattice and reduces stiffness [14].

Graphene is a two-dimensional (2D) multifunctional nanomaterial with a high specific surface area, high specific strength and high conductivity [15–17]. The properties of graphene composites have been widely explored. For example, the addition of graphene and a new class of three-dimensional (3D) graphene improves the fatigue performance of epoxy resin [18]. Similarly, 3D graphene enhances the buckling resistance of glass fibre composites [19], and 2D graphene significantly increases the mechanical properties (tensile modulus and strength, flexural and impact strength) of glass fibre-reinforced composites with different lay-up methods [20]. However, the effect of graphene on the mechanical properties of FMLs is poorly understood [21].

The usefulness of graphene gives versatility to its composites. The electrical properties of graphene composites are often discussed [22,23]. For instance, the influence of graphene on the electrical properties of epoxy resins has been investigated through experiments and numerical modelling, which reveal that the electrical conductivity of epoxy can be effectively improved by graphene [23]. It has a similar effect on cement-based composites [22]. The improved conductivity of composites is conducive to the realisation of structural health monitoring (SHM). Monitoring damage through changes in electrical signals has become an essential means of SHM. The more common ones are impedance-based applications [24–26]. With the particular structure of FMLs, SHM can be completed with capacitive signals [27,28]. Therefore, the electrochemical performance of FMLs with graphene should be further explored.

Considering the balance of mechanical performance and electrical conductivity for SHM, this study investigates the effect of different graphene mass ratios (0 wt.%,

0.2 wt.%, 0.3 wt.%, 0.5 wt.% and 1.0 wt.%) on the mechanical and electrochemical properties of GLARE. It compares the test results to understand the influence of different graphene contents on structural properties. It also analyses the microscopic morphology of the structure through scanning electron microscopy (SEM) to explain the obtained results. Our results provide a basis for enhancing the mechanical properties of GLARE and conducting an *in situ* damage inspection of structures without sacrificing mechanical properties.

2. Experimental methods

2.1. Materials

GLARE laminates were adhered to alternate layers of two sheets: 0.3 mm-thick aluminium sheets (Al 2024; KAISER Co., USA) and 0.11 mm-thick glass fibre EW100 (Shanghai Yaohong Glass Fibre Co., China). Epoxy resin (Ciba-Geigy, Australia) was used as an adhesive with a Jeffamine D230 hardener (Huntsman). Filler graphene was prepared from a graphite intercalation compound (GIC, Asbury 1395; Asbury Carbons, Asbury, NJ, USA). Na_2SO_4 (Tianjin Hengxing Chemical Reagent Manufacturing Co., Ltd., Tianjin, China) was utilised as an electrolyte.

The tensile and flexural tests of the composite specimens were performed using an MTS E45.105 computer-controlled electronic universal testing machine under ASTM D3039, ASTM D790, respectively. Scanning electron microscopy (SU3500 SEM; Japan) was performed. An electrochemical workstation (ChenHua CHI660E B19038; Shanghai, China) was used to measure the electrochemical performance of the specimens.

2.2. Fabrication of graphene-reinforced GLARE

The graphene intercalation compound can form a thin layer of graphene platelets (GnPs) after thermal shock and ultrasonic treatment [29]. An effective preparation method for graphene-reinforced epoxy was described as follows. Graphene was dispersed in an acetone solution and sonicated for 120 min. Epoxy resin was added and sonicated for 60 min to disperse the nanofillers uniformly and connect graphene and epoxy molecules. Both steps were performed at 25 °C. Magnetic stirring was carried out at 70 °C to remove acetone. Then, the J230 hardener was added and mixed well after the specimens were cooled. Thus, a graphene/epoxy resin adhesive was obtained. The preparation process is shown in Figure 1(a), and metal surface treatment and GLARE formation are illustrated in Figure 1(b). The metal surfaces were chemically etched; the smooth metal surfaces became rough and formed a cubic morphology [30]. Afterwards, the adhesive hand lay-up was used to obtain graphene-enhanced GLARE, whose fibres were orthogonal. The stacking sequences of the glass fibre and the aluminium alloy were manufactured through compression moulding [31], which involved two steps. Firstly, a vacuum bag was sealed to form a vacuum environment. Secondly, an autoclave was heated and pressurised for curing. The curing temperature and pressure curve are presented in Figure 1(c).

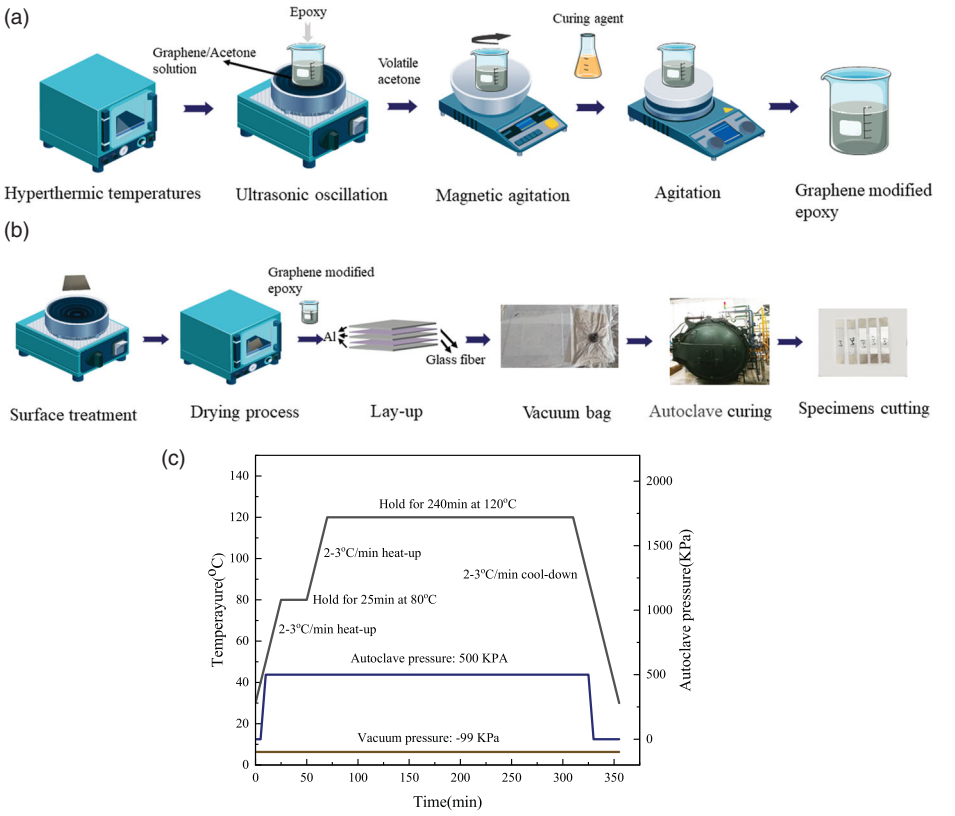

Figure 1. Schematic diagram of the specimens preparation process (a) the fabrication process of epoxy with graphene, (b) fabrication process of the GLARE specimens, and (c) the curing curves of GLARE.

2.3. Mechanical performance test and morphologies

The conducted GLARE specimens comprised three different tests: tensile testing, flexural testing and electrochemical property testing. In a three-point flexural test, different span length-to-specimen thickness (L/h) ratios (8/1 and 32/1) have different ILSS and flexural strength values [32–34]. In our study, the dimensions of the tensile test specimens were 250 mm × 25 mm, and the loading rate was 2.0 mm/s. The width was 10 mm, and the lengths were 20 (8/1) and 50 mm (32/1). Stress and strain signals were obtained using the testing machine. The following equations were used to calculate flexural strength and ILSS:

$$\text{Flexural strength}: \quad \sigma_f = \frac{3FL}{2bh^2} \tag{1}$$

$$\text{ILSS} \quad : \sigma_i = \frac{3F}{4bh} \tag{2}$$

where σ_f is the flexural strength of GLARE (MPa), σ_i is the ILSS of GLARE (MPa), F is the first peak load in the flexural tests (N), L is the support span (mm), and b and h are

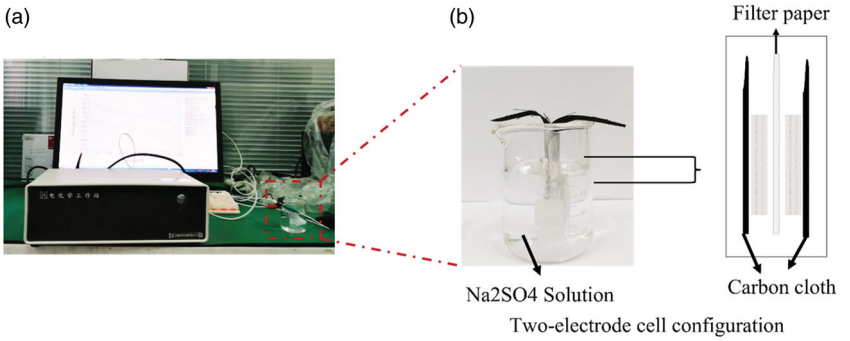

Figure 2. (a) The electrochemical workstation, (b) electrochemical test schematic.

the average width and thickness of the GLARE specimen (mm), respectively. SEM was conducted to characterise the surface morphology of the metal and fibre of the GLARE specimens.

2.4. Electrochemical performance test

In the electrochemical test (Figure 2), graphene-modified GLARE was used as an electrode. Double electrodes, double carbon cloth and filter paper for isolation were tested in a two-electrode cell configuration. Signals were collected through an electrochemical workstation. Specific capacitance was calculated as follows [35].

$$C_s = \frac{1}{m \cdot \Delta v \cdot v} \int_{v_-}^{v_+} L(v)dv \tag{3}$$

where v is the scan speed (V/s), Δv is the operating voltage (V), and m is the electrode active material quality (about 0.0008 g).

3. Results and discussion

3.1. Tensile strength

The effect of different graphene quantities on the tensile properties of GLARE is tested and compared. When FMLs are subjected to tensile load, the main force-bearing elements are the fibre composite layer and the metal layer, the structure interface, is often a weakness [36,37]. Under the tensile process, the stress-strain curves of GLARE with different graphene quantities (0 wt.%, 0.2 wt.%, 0.3 wt.%, 0.5 wt.% and 1.0 wt.%; Figure 3) indicate a non-linear relationship between stress and strain. Inflexion points exist in the curves of different graphene quantities. The slopes of the stress-strain course before and after the inflexion point are different. Only elastic deformation occurs before the inflexion point is reached; the yield and plastic deformation of the aluminium layer are the main reasons for the inflexion point. After the inflexion point, the aluminium layer completely forms, and only the glass fibre layer undergoes elastic deformation until failure takes place [37].

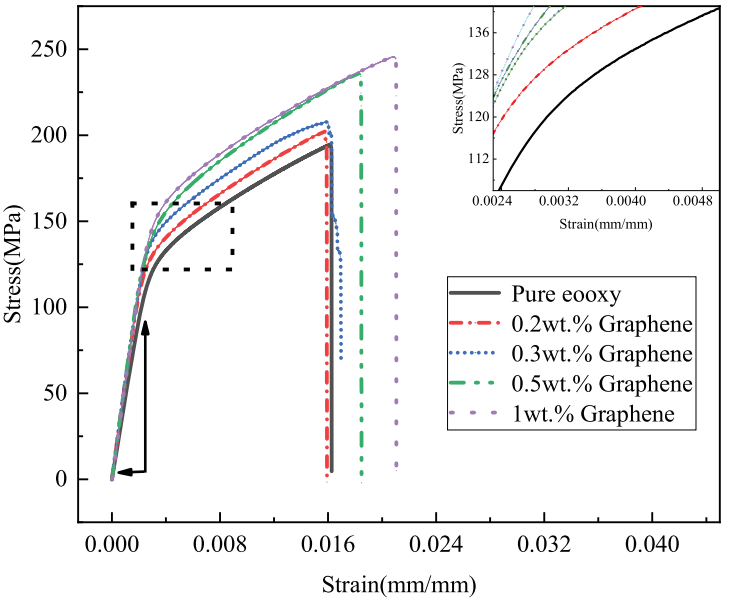

Figure 3. The stress-strain curves of GLARE of different graphene quantities.

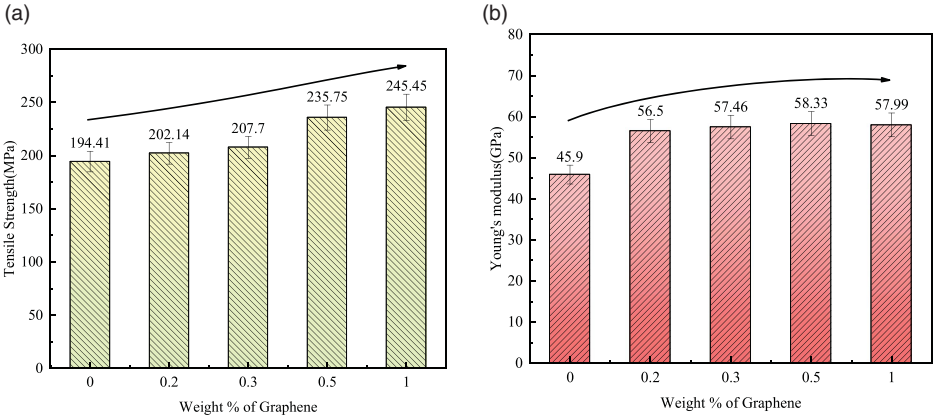

Figure 4. Tensile test results of graphene reinforced GLARE, (a) Tensile strength, (b) Young's modulus.

Table 1. The tensile properties of the graphene reinforced GLARE specimens.

Graphene wt.%	Tensile strength (MPa)	Increment (%)	Young's modulus (GPa)	Increment (%)
0	194.41 ± 9.72	0	45.9 ± 0.97	0
0.2	202.14 ± 10.11	3.98	56.5 ± 0.73	23.09
0.3	207.7 ± 10.385	6.84	57.46 ± 0.65	25.19
0.5	235.75 ± 11.79	21.26	58.33 ± 0.55	27.08
1	245.45 ± 12.27	26.25	57.99 ± 0.48	26.34

Figure 4 and Table 1 show the tensile properties, including tensile strength and Young's modulus, of graphene-enhanced GLARE according to ASTM D3039. They are two important parameters that characterise the tensile properties of composites [38–40]. Graphene (in wt.%) introduction increases the tensile strength and Young's

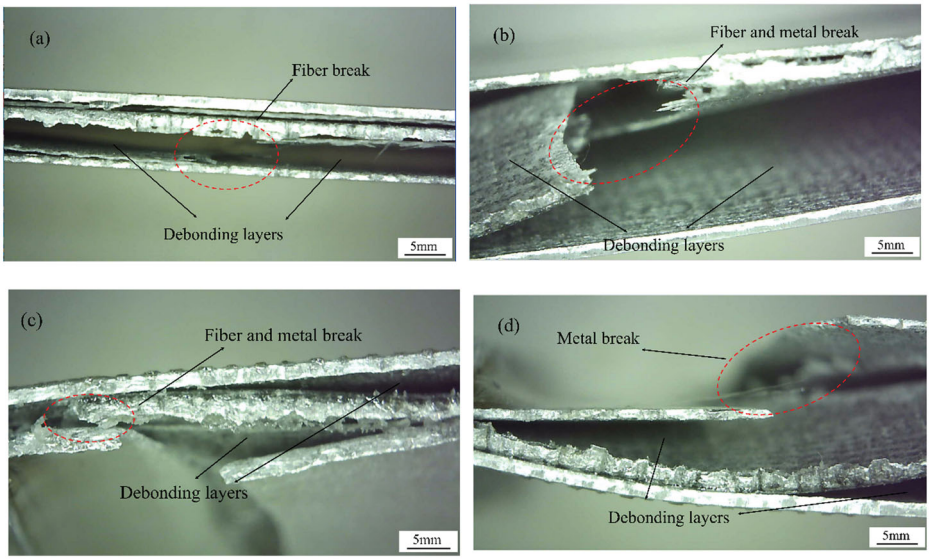

Figure 5. Failure modes of GLARE, (a) pure epoxy, (b) 0.2 wt.% graphene, (c) 0.5 wt.% graphene, (d) 1.0 wt.% graphene.

modulus of GLARE (Figure 3). However, they exhibit different trends. With graphene addition (0 wt.%–1.0 wt.%), the tensile strength continuously enhances, as illustrated in Figure 4(a). When the graphene content is 1.0 wt.%, the maximum tensile strength of the specimens is 245.45 ± 12.27 MPa (26.25% larger than pure epoxy GLARE). In Figure 4(b), Young's modulus as a function of graphene content initially increases, slowly decreases, and peaks at 0.5 wt.% of graphene filler. The maximum is 58.33 ± 0.55 GPa (27.08% higher than pure epoxy GLARE). These results are similar to previous findings [41,42].

The improved tensile properties of the sample after graphene modification compared with those of pure epoxy GLARE are mainly attributed to glass fibre-reinforced composite layers. Under uniaxial tensile loadings, cracks mainly form in the resin matrix, and the sample expands laterally. This phenomenon further evokes the debonding of fibres; it also causes the breakage of the matrix, fibre and metal and induces delamination between the fibre and the metal layer (Figure 5). The form of failure changes significantly. From fibre break to fibre and metal break together, graphene content ranges from 0 wt.% to 0.5 wt.%. When the graphene content increases to 1.0 wt.%, the fibre layer is sufficiently reinforced, and its fracture no longer occurs, but the metal layer becomes fractured.

Graphene addition changes the crack propagation in the fibre layer. Graphene forms a mechanical interlock between the fibre and the epoxy resin to increase the strength of the fibre layer. In crack propagation, cracks generally grow along the boundary between graphene and epoxy, thereby increasing the distance of crack propagation. If they pass through graphene, graphene is pulled out of the resin matrix [43]. The above phenomena absorb more energy and inhibit crack growth. Graphene addition also enhances matrix cracking, fibre–matrix debonding, fibre pull-out and fibre rupture [41]. By contrast, the interlayer strength of the metal and glass fibre layers of graphene

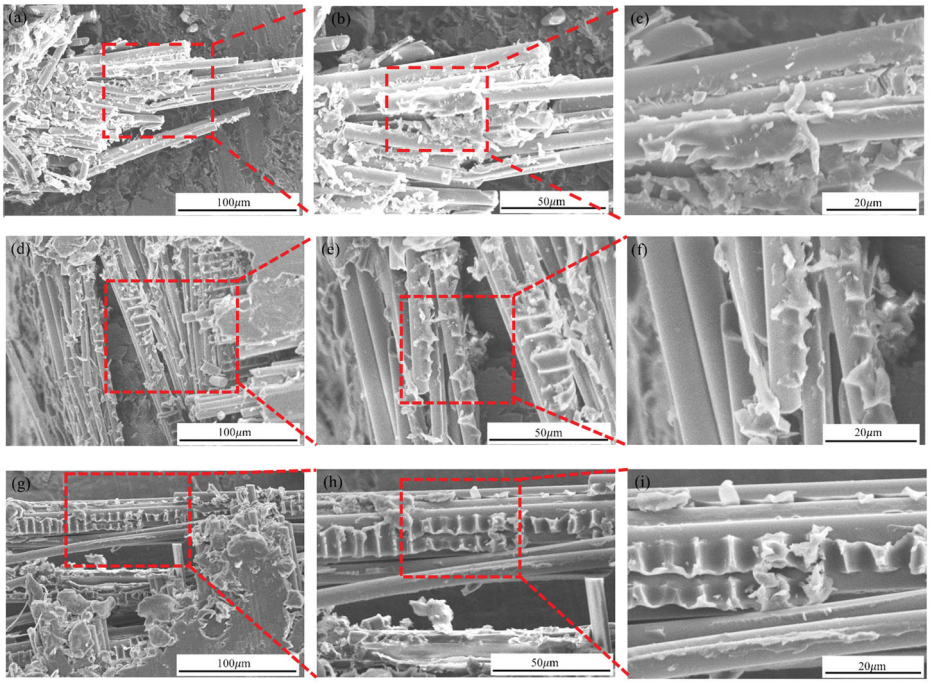

Figure 6. SEM image of tensile specimen, (a–c) 0.2 wt.% graphene, (d–f) 0.5 wt.% graphene, (g–h) 1.0 wt.% graphene.

during stretching is less obvious. Therefore, the tensile properties of GLARE can be further enhanced by reinforcing the glass fibre layer.

Figure 6 shows the SEM image of the tensile specimens of GLARE modified with 0.2 wt.% (a)–(c), 0.5 wt.% (d)–(f) and 1.0 wt.% (g)–(i) graphene. In Figure 6(a), when the graphene content is low (0.2 wt.%), the fibre breakage has a whisker-like morphology, which indicates that the bond between the fibre and the matrix is weak under these circumstances. When the graphene content increases (0.5 wt.% and 1.0 wt.%), the fibre breaks become evenly distributed, as shown in Figures 6(d,g), because graphene addition enhances the interface bonding force. As presented in Figures 6(c,f,i), this phenomenon is attributed to graphene involvement in the breakage of fibres and the debonding of fibres and resin through a mechanical linkage. According to the energy dissipation concept of an interface failure, cracks consume energy during expansion, and graphene increases this energy. Before graphene massively agglomerates, this enhancement continues to increase as the graphene content increased.

3.2. Flexural properties

Flexural performance is the manifestation of the comprehensive performance of GLARE laminates include tension, compression and shear. Therefore, the bending strength of GLARE depends on which of the three stresses of the specimen reaches the limit value first [44]. As indicated in Figure 7, graphene improves the flexural resistance of GLARE laminates. Figure 7(a) presents the results from three-point bending

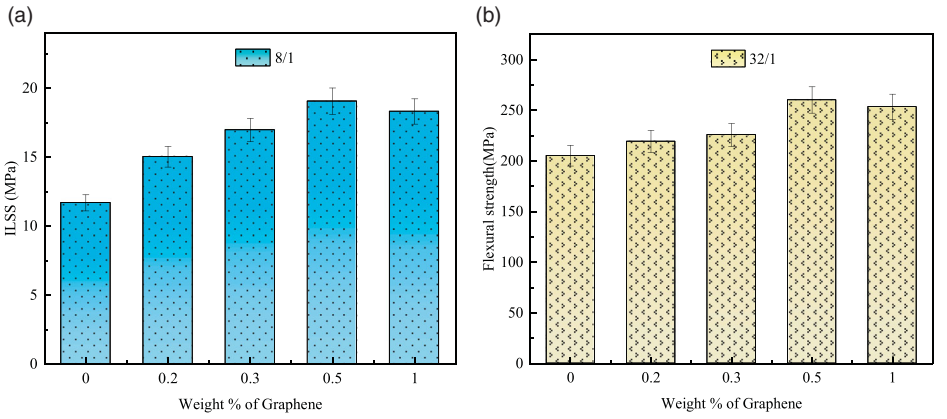

Figure 7. Test results of short-beam three-point-bending load (a) ILSS (L/*h* = 8/1), (b) Flexural strength (L/*h* = 32/1) of the graphene reinforced GLARE.

Table 2. Flexural strength and ILSS of the graphene reinforced GLARE.

Graphene wt.%	ILSS (MPa)	Increment (%)	Flexural strength (MPa)	Increment (%)
0	11.69 ± 0.58	0	205.26 ± 10.26	0
0.2	15.03 ± 0.75	28.57	219.33 ± 10.94	6.85
0.3	16.97 ± 0.85	45.17	225.74 ± 11.29	9.98
0.5	19.06 ± 0.95	63.05	260.22 ± 13.01	26.78
1	18.31 ± 0.92	56.63	253.37 ± 12.67	23.44

when L/h is 8/1; thus, ILSS is obtained. A short-beam shear test provides practical information about ILSS, which characterises the interlaminar resistance of GLARE [34]. The reason is that when GLARE is subjected to a three-point bending load, the form of loading stress changes with L/h [33]. When L/h is 8/1, the specimen is mainly subjected to shear stress [32], as illustrated in Figure 7(b), when L/h is 32/1, the specimens are mainly subjected to flexural stress [32,36].

Although the stress loads are different, the effects of graphene on the two cases have many similarities. The specific flexural performance is shown in Table 2. For example, as the graphene content increases, ILSS and flexural strength gradually increase, and the enhanced peak value is the same (0.5 wt.%). After this phase, they decrease. However, the performance at this time (1 wt.%) is still higher than that of pure epoxy specimens mainly because the increase in graphene content causes agglomeration and affects its mechanical properties. Graphene agglomeration affects the mechanical properties at a lower mass ratio than that in the aforementioned tensile experiment. Therefore, different mechanical behaviours have various degrees of tolerance to graphene agglomeration.

The failure modes of the specimens under two stress loadings are extremely different from each other. The load is bending stress when L/h is 32/1, so the graphene filler does not affect the failure form of the specimens, as shown in Figures 8(e–h). For specimens with shear stress, the failure mode changes significantly, as shown in Figures 8(a–d). Pure epoxy GLARE mainly exists during fibre and metal fracture and debonding delamination (Figure 8). Furthermore, 0.2 wt.% graphene-enhanced GLARE is similar. The continuous increase in graphene content (0.3 wt.%) strengthens the fibre layer, and failure begins to be dominated by delamination. When the mass ratios of

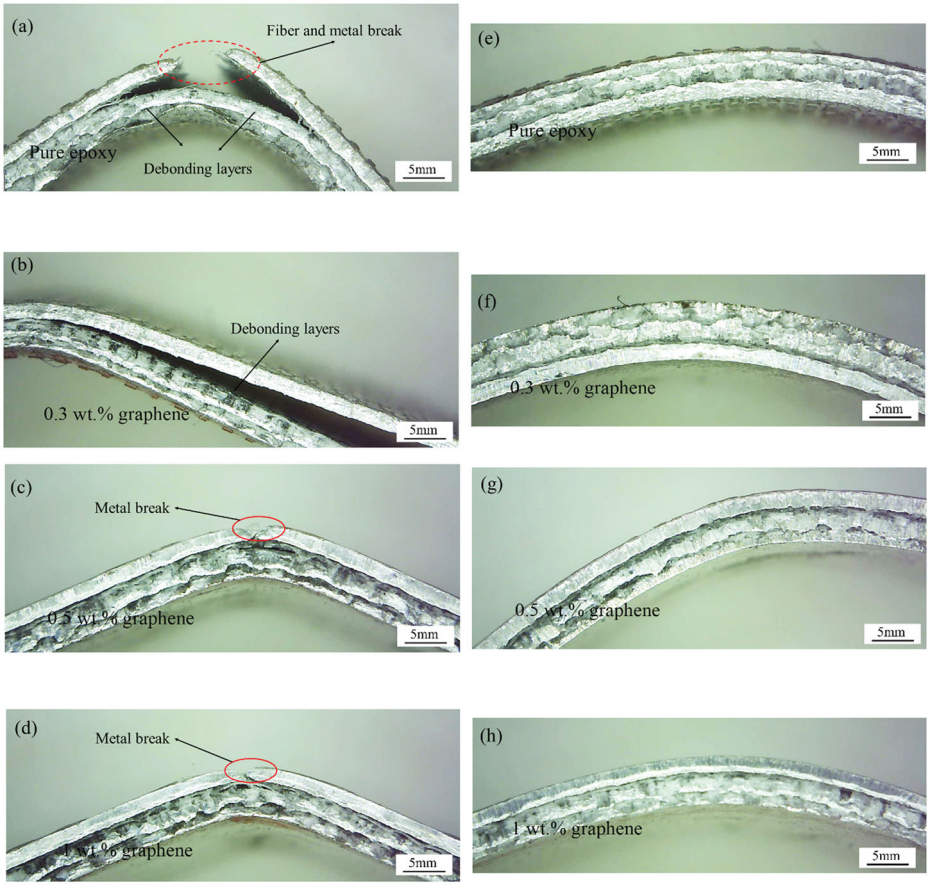

Figure 8. The failure mode of the pure epoxy GLARE and 0.3 wt.%, 0.5 wt.%, 1.0 wt.% graphene-GLARE, (a–d) L/h is 8/1, (e–h) L/h is 32/1.

graphene are 0.5 wt.% and 1.0 wt.%, delamination disappears, and the failure form is metal destruction. Therefore, ILSS reaches its highest point at 0.5 wt.% graphene.

For the graphene-modified GLARE, the interlayer performance is improved mainly in three aspects: the shear resistance of the epoxy matrix, the force transmission capacity between the fibre and the epoxy and the adhesion between the epoxy and the metal surface [10]. Therefore, under the bending load, the ILSS and failure mode of the graphene-modified GLARE change.

The variability in the failure form of GLARE specimens means that graphene simultaneously enhances the fibre layer and interlayer of fibre/metal strength during the bending test. This result is different from the tensile experiment. Figure 9 shows the microscopic morphology of the aluminium surface of a flexural specimen with a lower graphene content (0 wt.% and 0.3 wt.%) when L/h is 8. Figure 9 also clearly illustrates the epoxy matrix, the aluminium surface and the clear dividing line. Delamination failure is caused by insufficient adhesion between the resin and the aluminium. Adding graphene to the matrix can increase the strength

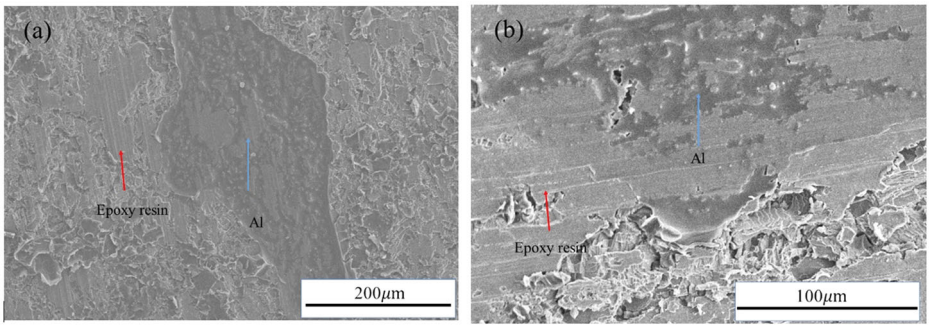

Figure 9. The micro-morphology of the aluminium surface with delamination, (a) pure epoxy GLARE, (b) 0.3 wt.% graphene reinforced GLARE.

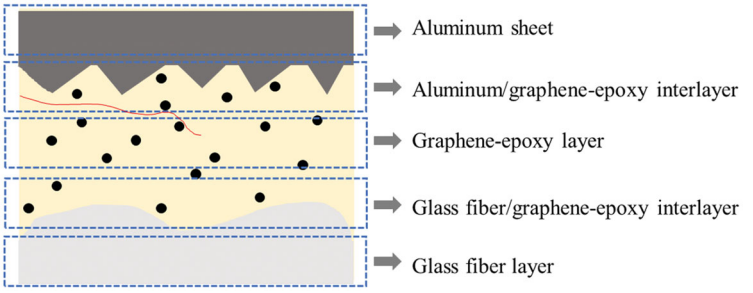

Figure 10. The cross-sectional view of the 0.5 wt.% graphene reinforced GLARE specimen.

of the adhesion. It also improves the interlayer performance of GLARE flexural specimens and changes the failure mode.

A schematic is shown to explain the above phenomenon and the mechanism of graphene-induced enhancement of the adhesion between the resin and aluminium. Figure 10 is a cross-sectional view of the 0.5 wt.% graphene-reinforced GLARE specimen when L/h is 8/1. A graphene-reinforced GLARE laminate structure has five different areas (Figure 10). The red line indicates crack growth. Two crack growth zone are interfaces, including aluminium/graphene-epoxy and glass fibre/graphene-epoxy interfaces.

Usually, cracks initially occur in aluminium/graphene-epoxy interlayer areas and expand in the aluminium/graphene-epoxy interlayer or graphene-epoxy layer areas. Graphene hinders crack propagation by forming a mechanical linkage with the resin matrix. When the crack propagation encounters the graphene sheet, the crack front is deflected or twisted (Figure 10), thereby increasing the surface area and energy absorption of the fracture [43]. Figure 11 shows a microscopic image of the fractured surface of the resin matrix with 0.5 wt.% graphene. The blue arrow in Figure 11(b) marks the pulled or broken graphene. This mechanical interlocking with the resin matrix is the main toughening mechanism of graphene. In this phenomenon, a high amount of energy is absorbed, and the strength of the adhesion between the resin and aluminium increases. The metal layer likely fails before the glass fibre/aluminium layer, and the result is obtained (Figure 9).

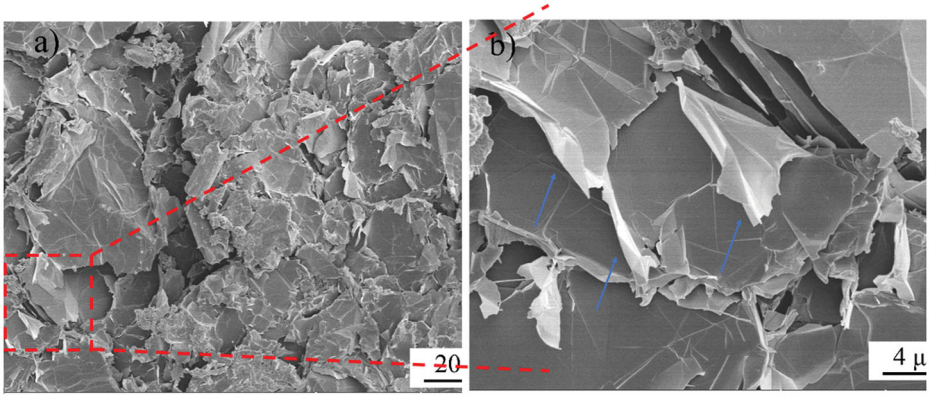

Figure 11. The microscopic image of the fractured surface with 0.5 wt.% graphene.

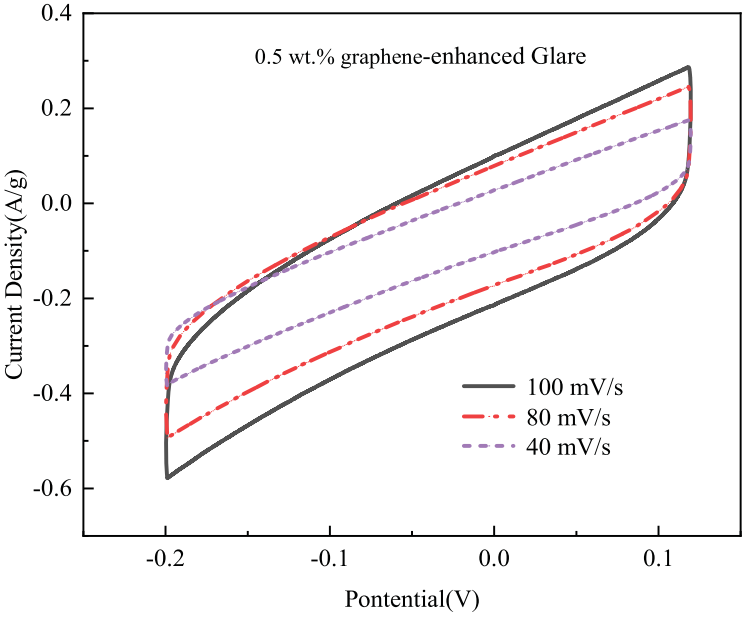

Figure 12. Electrochemical characteristics of GLARE composites modified by 0.5 wt.% graphenes.

3.3. Capacitance properties

In Subsection Flexural properties, the influence of graphene on the flexural performance of GLARE is discussed. The results show that the best component is 0.5 wt.%. In this subsection, 0.5 wt.% graphene-enhanced GLARE is further discussed. The excellent electrochemical properties of graphene provide the electrochemical properties of graphene/composite.

In the electrochemical workstation, the capacitance performance of the 0.5 wt.% graphene-enhanced GLARE laminate is tested with a two-electrode cell configuration. The CV curves of graphene/composites at different scan rates (40, 80, and 100 mV/s) are shown in Figure 12. Under different scan rates, similar trends and shapes are observed in the CV curves. These results indicate that the modified GLARE shows superior

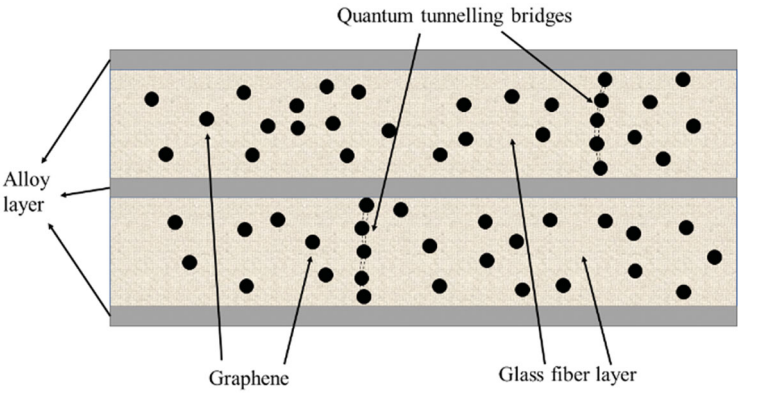

Figure 13. Graphene particles form a quantum tunneling model.

electrochemical performance [45]. Equation (3) describes the calculation method and principle. The specific capacitance values corresponding to the scan rates of 40, 80, and 100 mV/s are 1.76, 2.47, and 2.88 F/g, respectively. Although this value is lower than that of supercapacitors [35,45], certain electrochemical characteristics are still detected.

A particle tunnelling model explains why conductive nanoparticles form a conductive network in a polymer to improve conductivity [46,47]. Figure 13 shows the quantum tunnelling model, and certain sections of the whole frame are appropriately scaled for clarity. Graphene is uniformly dispersed in epoxy resin and forms a conductive network (Figure 13). Thus, the modified GLARE adsorbs more ions on the surface when it is used as an electrode. As such, the structure containing nonconductive glass fibres exhibits electrochemical properties.

4. Conclusion

This study explores the influence of different graphene contents (0 wt.%, 0.2 wt.%, 0.3 wt.%, 0.5 wt.% and 1.0 wt.%) on the performance of GLARE in terms of its tensile, flexural and electrochemical properties. The results indicate that the flexural and tensile properties of GLARE are increased by graphene platelets to varying degrees in terms of mechanical strength and failure modes. The mechanical behaviour of the graphene-reinforced GLARE enhances, and a certain electrochemical performance can be obtained.

Graphene enhances the overall strength of GLARE by increasing the strength of the glass fibre composite layer. The tensile strength and Young's modulus of GLARE improve by 26.25% and 27.08% with continuous graphene addition (0 wt.%–1.0 wt.%). Graphene addition can also change the failure mode of GLARE specimens. In summary, when the quality of graphene is relatively low (0 wt.%–0.5 wt.%), metal and fibre almost become damaged and delaminated. When the graphene mass ratio is 1.0 wt.%, fibre destruction disappears, and metal damage and delamination cause the failure of the graphene-reinforced GLARE specimens.

The bending performance under the two different L/h ratios sufficiently improves and peaks when the graphene content is 0.5 wt.%. If the graphene content continues to increase, the performance of graphene decreases because of the agglomeration of excess

graphene. Furthermore, the tolerance of bending performance to this phenomenon is different from that of tensile performance. When L/h is 8, graphene improves the performance between metal and fibre layers. This observation also differs from the results of the tensile experiment.

When the bending strength peaks (0.5 wt.% graphenes), GLARE has certain electrochemical properties. The specific capacitance values at scan rates of 40, 80, and 100 mV/s are 1.76, 2.47, and 2.88 F/g, respectively, mainly because graphene forms a conductive network in the resin matrix; consequently, GLARE can absorb more ions. Thus, this study provides a basis for monitoring the structural health of GLARE.

Disclosure statement

No potential conflict of interest was reported by the authors.

Funding

This work was financially supported by the Aeronautical Science Foundation of China [2020Z055054002 and 2018ZF54036], National Natural Science Foundation [51973123], Natural Science Foundation of Liaoning Province (2019-MS-256), the Scientific Research Funds from Liaoning Education Department (JYT2020007), Training Project of Liaoning Higher Education Institutions (No. 2018LNGXGJWPY-YB008) and Liaoning Province Natural Fund Project (No. 2019-ZD-0246).

ORCID

Sherif Araby http://orcid.org/0000-0001-6807-7926
Qingshi Meng http://orcid.org/0000-0002-8187-7028

References

[1] van Rooijen RGJ, Sinke J, van der Zwaag S. Improving the adhesion of thin stainless steel sheets for fibre metal laminate (FML) applications. J Adhes Sci Technol. 2005; 19(16):1387–1396.
[2] Thirukumaran M, Jappes JTW, Siva I, et al. On the interfacial adhesion of fiber metal laminates using surface modified aluminum 7475 alloy for aviation industries – a study. J Adhes Sci Technol. 2020;34(6):635–650.
[3] Lin Y, Liu C, Li H, et al. Interlaminar failure behavior of GLARE laminates under double beam five-point-bending load. Compos Struct. 2018;201:79–85.
[4] Deniz ME, Aydin F. Determination of fatigue life of the unidirectional GFRP/Al hybrid composite laminates. Composites Part B: Engineering. 2019;166:580–587.
[5] Wang Z, Zhao J. Low velocity impact response of GLARE laminates based on a new efficient implementation of puck's criterion. Thin-Walled Structures. 2019;144:106321.
[6] Kwon D-J, Shin P-S, Kim J-H, et al. Interfacial properties and thermal aging of glass fiber/epoxy composites reinforced with SiC and SiO2 nanoparticles. Composites Part B: Engineering. 2017;130:46–53.
[7] Zhang X, Hu Y, Li H, et al. Effect of multi-walled carbon nanotubes addition on the interfacial property of titanium-based fiber metal laminates. Polym Compos. 2018; 39(S2):E1159–E1168.

[8] Meng Q, Han S, Liu T, et al. Noncovalent modification of boron nitrite nanosheets for thermally conductive, mechanically resilient epoxy nanocomposites. Ind Eng Chem Res. 2020;59(47):20701–20710.
[9] Megahed M, Abd El-Baky MA, Alsaeedy AM, et al. An experimental investigation on the effect of incorporation of different nanofillers on the mechanical characterization of fiber metal laminate. Composites Part B: Engineering. 2019;176:107277.
[10] Li L, Lang L, Khan S, et al. Investigation into effect of the graphene oxide addition on the mechanical properties of the fiber metal laminates. Polym Test. 2020;91:106766.
[11] Wu X, Ning H, Liu Y, et al. Synergistic delamination toughening of glass Fiber-Aluminum laminates by surface treatment and graphene oxide interleaf. Nanoscale Res Lett. 2020;15(1):74–74.
[12] Han S, Meng Q, Chand A, et al. A comparative study of two graphene based elastomeric composite sensors. Polym Test. 2019;80:106106.
[13] Han S, Meng Q, Pan X, et al. Synergistic effect of graphene and carbon nanotube on lap shear strength and electrical conductivity of epoxy adhesives. J Appl Polym Sci. 2019;136(42):48056.
[14] Li Z, Kinloch IA, Young RJ. The role of interlayer adhesion in graphene oxide upon its reinforcement of nanocomposites. Philos Trans A Math Phys Eng Sci. 2016;374(2071): 20150283.
[15] Gedler G, Antunes M, Velasco JI. Enhanced electrical conductivity in graphene-filled polycarbonate nanocomposites by microcellular foaming with sc-CO2. J Adhes Sci Technol. 2016;30(9):1017–1029.
[16] Dong J, Jia C, Song Y, et al. Improved interfacial properties of carbon fiber-reinforced epoxy composites with Fe2O3/graphene nanosheets using a magnetic field. J Adhes Sci Technol. 2018;32(9):1018–1026.
[17] Hülagü B, Ünal HY, Acar V, et al. Low-velocity impact and bending response of graphene nanoparticle-reinforced adhesively bonded double strap joints. J Adhes Sci Technol. 2021;:1–19.
[18] Kordi A, Adibnazari S, Imam A, et al. Effects of two- and three-dimensional graphene-based nanomaterials on the fatigue behavior of epoxy nanocomposites. Mater Today Commun. 2020;24:101194.
[19] Asaee Z, Mohamed M, Soumik S, et al. Experimental and numerical characterization of delamination buckling behavior of a new class of GNP-reinforced 3D fiber-metal laminates. Thin-Walled Structures. 2017;112:208–216.
[20] Mishra BP, Mishra D, Panda P, et al. An experimental investigation of the effects of reinforcement of graphene fillers on mechanical properties of bi-directional glass/epoxy composite. Mater Today: Proc. 2020;33:5429–5441.
[21] Shen C, Oyadiji SO. The processing and analysis of graphene and the strength enhancement effect of graphene-based filler materials: a review. Materials Today Physics. 2020; 15:100257.
[22] Yoo D-Y, You I, Lee S-J. Electrical properties of cement-based composites with carbon nanotubes, graphene, and graphite nanofibers. Sensors. 2017;17(5):1064.
[23] Han S, Meng Q, Araby S, et al. Mechanical and electrical properties of graphene and carbon nanotube reinforced epoxy adhesives: experimental and numerical analysis. Composites Part A: Applied Science and Manufacturing. 2019;120:116–126.
[24] Meng Q, Han S, Araby S, et al. Mechanically robust, electrically and thermally conductive graphene-based epoxy adhesives. J Adhes Sci Technol. 2019;33(12):1337–1356.
[25] Han S, Chand A, Araby S, et al. Thermally and electrically conductive multifunctional sensor based on epoxy/graphene composite. Nanotechnology. 2020;31(7):075702.
[26] Han S, Zhang X, Wang P, et al. Mechanically robust, highly sensitive and superior cycling performance nanocomposite strain sensors using 3-nm thick graphene platelets. Polym Test. 2021;98:107178.
[27] Yan J, Downey A, Chen A, et al. Capacitance-based sensor with layered carbon-fiber reinforced polymer and titania-filled epoxy. Compos Struct. 2019;227:111247.

[28] Bosbach B, Ohle C, Fiedler B. Structural health monitoring of fibre metal laminates under mode I and II loading. Composites Part A: Applied Science and Manufacturing. 2018;107:471–478.
[29] Zaman I, Kuan H-C, Dai J, et al. From carbon nanotubes and silicate layers to graphene platelets for polymer nanocomposites. Nanoscale. 2012;4(15):4578–4586.
[30] Zamani Zakaria A, Shelesh-Nezhad K, Navid Chakherlou T, et al. Effects of aluminum surface treatments on the interfacial fracture toughness of carbon-fiber aluminum laminates. Eng Fract Mech. 2017;172:139–151.
[31] Khalid MY, Arif ZU, Sheikh MF, et al. Mechanical characterization of glass and jute fiber-based hybrid composites fabricated through compression molding technique. Int J Mater Form. 2021;14(5):1085–1095.
[32] Liu C, Du D, Li H, et al. Interlaminar failure behavior of GLARE laminates under short-beam three-point-bending load. Composites Part B: Engineering. 2016;97:361–367.
[33] Khalid MY, Arif ZU, Al Rashid A, et al. Interlaminar shear strength (ILSS) characterization of fiber metal laminates (FMLs) manufactured through VARTM process. Forces in Mechanics. 2021;4:100038.
[34] Khalid MY, Al Rashid A, Sheikh MF. Effect of anodizing process on inter laminar shear strength of GLARE composite through T-Peel test: experimental and numerical approach. Exp Tech. 2021;45(2):227–235.
[35] Cymann A, Sawczak M, Ryl J, et al. Capacitance enhancement by incorporation of functionalised carbon nanotubes into poly(3,4-Ethylenedioxythiophene)/graphene oxide composites. Materials. 2020;13(10):2419.
[36] Sun J, Daliri A, Lu G, et al. Tensile failure of fibre-metal-laminates made of titanium and carbon-fibre/epoxy laminates. Materials & Design. 2019;183:108139.
[37] Hu Y, Zhang Y, Fu X, et al. Mechanical properties of Ti/CF/PMR polyimide fiber metal laminates with various layup configurations. Compos Struct. 2019;229:111408.
[38] Nagaraj C, Mishra D. Estimation of tensile properties of fabricated multi layered natural jute fiber reinforced E-glass composite material. Mater Today: Proc. 2020;27:1443–1448.
[39] Chen J, Yan Y, Mei H, et al. Enhancing the tensile properties of SiC composites by a two-dimensional CNT film. Ceram Int. 2021;47(3):4111–4117.
[40] Ashik KP, Sharma RS. Evaluation of tensile, modal and fracture properties of jute/epoxy natural composites with addition of silicon Di oxide as filler material. Mater Today: Proc. 2017;4(9):9586–9591.
[41] Adak NC, Chhetri S, Kim NH, et al. Static and dynamic mechanical properties of graphene oxide-incorporated woven carbon fiber/epoxy composite. J Materi Eng Perform. 2018;27(3):1138–1147.
[42] Díez-Pascual A, Ashrafi, B M. Influence of carbon nanotubes on the thermal, electrical and mechanical properties of poly(ether ether ketone)/glass fiber laminates. Carbon. 2011;49(8):2817–2833.
[43] Du X, Zhou H, Sun W, et al. Graphene/epoxy interleaves for delamination toughening and monitoring of crack damage in carbon fibre/epoxy composite laminates. Compos Sci Technol. 2017;140:123–133.
[44] Caminero MA, Rodríguez GP, Muñoz V. Effect of stacking sequence on charpy impact and flexural damage behavior of composite laminates. Compos Struct. 2016;136:345–357.
[45] Cui X, Tian J, Yu Y, et al. Multifunctional graphene-based composite sponge. Sensors. 2020;20(2):329.

[46] Lin L, Liu S, Zhang Q, et al. Towards tunable sensitivity of electrical property to strain for conductive polymer composites based on thermoplastic elastomer. ACS Appl Mater Interfaces. 2013;5(12):5815–5824.
[47] Paredes-Madrid L, Matute A, Bareño J, et al. Underlying physics of conductive polymer composites and force sensing resistors (FSRs). A study on creep response and dynamic loading. Materials. 2017;10(11):1334.